

## Scaling laws in granular flows down a rough plane

B. Andreotti, A. Daerr, and S. Douady

Laboratoire de Physique Statistique de l'ENS, 24 rue Lhomond, 75231 Paris CEDEX 05, France

(Received 20 July 2000; accepted 17 September 2001)

The scaling properties of granular flows down an inclined plane are investigated in a model previously proposed to describe surface flows on a sandpile. Introducing a depth dependent friction, we are able to reproduce the results obtained experimentally by Pouliquen [Phys. Fluids **11**, 542 (1999); **11**, 1956 (1999)] on both the fronts velocities and their shapes. © 2002 American Institute of Physics. [DOI: 10.1063/1.1416884]

In two recent articles,<sup>1,2</sup> Pouliquen has shown experimentally that granular avalanches down an inclined plane covered by glued beads exhibit a robust scaling law, valid for various systems of beads and various plane roughness. This scaling indicates that the only characteristic length scale is the thickness  $Z_{\text{stop}}(\varphi)$  remaining when the flow stops (Fig. 1 and Refs. 3, 4). Despite its simplicity, this scaling has not yet received any theoretical explanation.

The rheology is interpreted by Pouliquen<sup>1,2</sup> as a flow in the whole height  $\zeta$  of the granular layer, whose mean velocity  $u$  scales as  $g^{1/2}\zeta^{3/2}/Z_{\text{stop}}(\varphi)$ . Since the maximum stable static height  $Z_{\text{stop}}(\varphi)$  is related to the increase of the effective friction close to the rough plane, this scaling law suggests that the velocity in the whole flowing layer is dominated by the rough plane effect and should thus be fundamentally different from the case of a flow at the surface of a sandpile. The experiment of Fig. 1 suggests an alternative picture: it reveals that there is, at least for a very rough bottom (velvet), a static layer of grains below the flowing one. This raises several questions: why does the friction force acting on the maximum static layer also control the rheology of the whole flowing layer? What actually occurs at the fixed boundary?

We have proposed a model<sup>5</sup> to describe granular flows at the surface of sandpiles, i.e., far from the bottom boundary. The aim of this letter is to compare the rheology obtained with our model, *a priori* not constructed for the case of a flow on a fixed bottom, to Pouliquen scaling law. A simplified version of our model is sufficient for this purpose.

The DAD model is based on Saint-Venant equations adapted to the case of a linear velocity profile (see Fig. 2 for notations). The variations of the velocity gradient  $\Gamma$  are determined from a "microscopic" dynamical model in which several flowing layers are inelastically coupled.<sup>6</sup> We have shown that  $\Gamma$  corresponds to the velocity of a single grain on a fixed grains layer.<sup>7</sup> In the latter case, the grain reaches a constant velocity  $\Gamma d$  which results from the balance between gravity and dissipation in the collisions.<sup>7,8</sup> An analytical approximation (Fig. 3, dashed line) of the observed variation of  $\Gamma$  with the surface angle  $\theta$  is

$$\Gamma = \beta \sqrt{\frac{g}{d}} \left/ \ln \left( \frac{\tan \theta_{\infty} - \tan \theta_0}{\tan \theta - \tan \theta_0} \right) \right. \quad (1)$$

The logarithmic cutoff at  $\theta_0$  corresponds to the trapping of the grain below this angle.<sup>7</sup> At  $\theta_{\infty}$ , the grain velocity diverges and above the grain constantly accelerates: when the centrifugal force becomes larger than gravity, it takes off and dissipates less and less in the collisions. With the above theoretical expression, the divergence angle is much too large compared to the experimental observation (last data point on Fig. 3) and the numerical findings.<sup>9</sup> A more accurate description is obtained by adding an upper unstable branch (Fig. 3, solid line): even below  $\theta_{\infty}$ , a grain can take off if pushed strongly enough and enter the accelerated regime.

We can now introduce this assumption of a linear velocity profile in Saint Venant conservation laws. The evolution of the free surface  $\zeta$  (Fig. 2) is governed by the conservation of matter:

$$\partial_t \zeta + \partial_x (\Gamma H^2/2) = 0, \quad (2)$$

where  $H$  is the thickness of the flowing layer. Under the assumption that the internal equilibrium fixes the velocity gradient  $\Gamma$ , the momentum  $q = \frac{1}{2}\Gamma H^2$  evolves with  $H$  due to the erosion/accretion process. Thus the momentum equation can be seen as an equation governing the evolution of the flowing height  $H$ :<sup>5</sup>

$$\partial_t H + \partial_x (\Gamma H^2/2) = \frac{g}{\Gamma} (\tan \theta - \mu(H)), \quad (3)$$

where  $\mu(H)$  is the friction acting on the layer and  $\tan \theta = -\partial_x \zeta$  is the free surface slope.  $\mu(H)$  is constructed to capture the hysteresis between the static and flowing states<sup>4,7,10</sup> (Fig. 4). Below a trapping height  $H_{\text{trap}}$ ,  $\mu(H)$  is equal to  $\mu_{\text{start}}$ , the slope above which grains spontaneously start to flow; above  $H_{\text{trap}}$ ,  $\mu(H)$  is equal to  $\mu_{\text{stop}}$ , the dynamical slope below which flows stop.  $H_{\text{trap}}$  is the typical flowing height under which the flow freezes even for a slope larger than  $\mu_{\text{stop}}$  and above which a perturbation amplifies to create an avalanche.<sup>4</sup>

To take into account the fact that the rough bottom spreads its influence inside the static grain layer up to several grains diameters,<sup>3,4</sup> the friction coefficients  $\mu_{\text{stop}}$  and  $\mu_{\text{start}}$  are assumed to depend exponentially on the position  $Z$  of the static/flowing interface with respect to the solid bottom (Fig. 5). Thus the friction force increases when going close to the rough plane meaning that the static layer is more and more

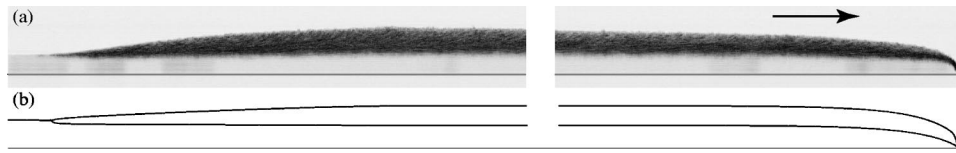


FIG. 1. (a) Experiment: side view of a dry granular flow down an inclined plane covered by velvet cloth. Right: a sharp front propagates at a constant velocity (from left to right on the figure), with a steady shape. Successive images difference reveals that the grains flow only on part of the total height (black), the rest (light gray) being static. Left: when the injection is suddenly stopped, a stopping front propagates downward (from left to right on the figure) leaving a uniform static layer of thickness  $Z_{stop}$  on the plane. The vertical scale is 10 times the horizontal one. (b) Model: the DAD model is integrated numerically for the same conditions. As in the experiment, the starting and stopping fronts propagate downward at two constant velocities.

difficult to mobilize. But *inside the flowing layer, the velocity gradient is assumed to be insensitive to the bottom plane*: its dependence with the free surface angle  $\theta$  remains controlled by the internal equilibrium between gravity driving and dissipation by collisions.<sup>6</sup>

To adjust our model parameters to Pouliquen's experiments, we first computed numerically the height  $Z_{stop}(\varphi)$  remaining on the plane when the flow stops (Fig. 5). As observed in Fig. 1(b) (left), a stopping front propagates down the plane which separates the flowing region from that perfectly at rest. The velocity of this front<sup>10</sup> is found to be nearly constant and equal to the velocity of one grain  $\Gamma d$ , while in the model it is found to be  $\Gamma H_{trap}$ ,<sup>11</sup> so that it corresponds to  $H_{trap}$  of the order of one grain diameter.<sup>4</sup> In first approximation  $Z_{stop}(\varphi)$  gives the dynamical friction coefficient  $\mu_{stop}(Z)$ :<sup>1,2,4</sup> when the flowing height is decreased,  $Z_{stop}$  is the first layer with enough friction to stop. It can be observed, however, that  $Z_{stop}(\varphi)$  is slightly larger than the dynamical friction coefficient  $\mu_{stop}(Z)$  (Fig. 5). This is due to the minimum flowing height  $H_{trap}$  (Fig. 4):  $Z_{stop}(\varphi)$  is roughly  $\mu_{stop}(Z)$  translated of  $H_{trap}$ . Note that this small  $H$  cutoff is necessary otherwise a stopping front would not be observed, but just an overall slowing down.<sup>11</sup> We also changed the control parameter to that of Pouliquen: instead of measuring the minimum flowing height at a given angle, we kept a constant surface height  $\zeta$  and decreased the angle to measure the angle  $\varphi_{stop}$  below which the flow stops. As in Pouliquen's experiment, the stopping height  $Z_{stop}(\varphi)$  and  $\varphi_{stop}(\zeta)$  nearly collapse (Fig. 5).

We can now turn to numerical simulations of Pouliquen's experiment, letting grains flow down an empty plane, and compare the front shapes.<sup>2</sup> Changing both the plane angle  $\varphi$  and the flow rate  $q_\infty$ , we observe that the slope of the front with respect to gravity remains the same (dotted

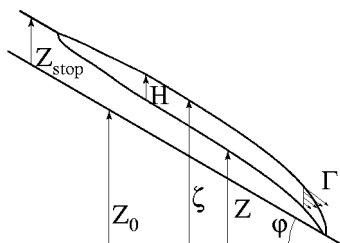


FIG. 2. In the model, the velocity profile inside the flowing granular layer is assumed to be linear, its vertical gradient being  $\Gamma$ . The local state of the sand pile is described by the flowing depth  $H$ , the free surface profile  $\zeta$  and by the position of the static/flowing interface  $Z = \zeta - H$ .

lines in Fig. 6). This property can also be deduced from the measurements and computations of Pouliquen.<sup>2</sup> It can be simply explained within our model. The material velocity at the surface is given by  $\Gamma H$  which *a priori* vanishes as  $H$  precisely at the front. If the material velocity at the front is null then the front can only sharpen. But as the slope increases, it reaches the value  $\theta_\infty$  (Fig. 3) for which  $\Gamma$  diverges. The velocity  $\Gamma H$  then becomes non-null, so that the front can propagate without further change of shape. Thus any propagating front present the same angle  $\theta_\infty$ , even for avalanches on a sandpile (Fig. 6,  $14^\circ$ ). With this constant slope at the front, it is natural that the surface profiles obtained for different flow rates at the same angle  $\varphi$  collapse on the same curve when rescaled by the overall height far from the front  $\zeta_\infty$  (Fig. 6,  $21^\circ$ ). As explained above, the divergence of  $\Gamma$  at  $\theta_\infty$  comes from the fact that the grains take off and form an accelerated gas. The model thus predicts the existence of a gaseous front and this is precisely what is observed in experiments. For instance, in Ref. 2 a picture shows few gaseous grains, enlightened by the laser sheet, ahead of the front. Again, this is not particular to fronts on a rough plane, but is also observed in avalanches at the surface of a sandpile.<sup>11</sup> In the rheology proposed by Pouliquen,<sup>2</sup> the front slope is also constant but its interpretation is quite different

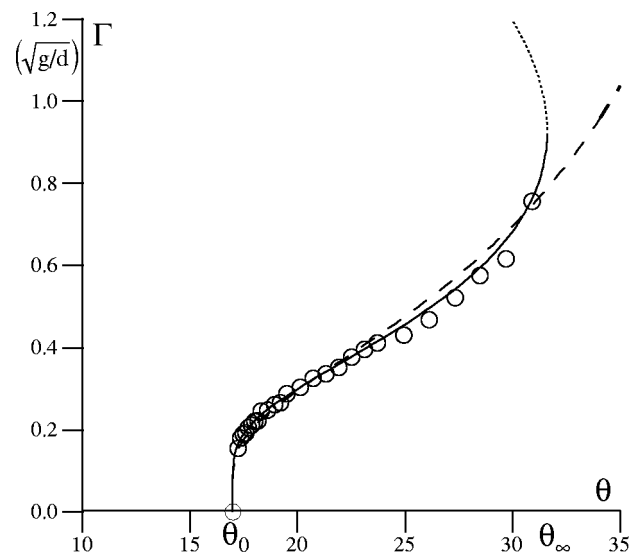


FIG. 3. The velocity gradient  $\Gamma$  for a slope  $\tan \theta$  is determined by the balance between gravity and dissipation by collisions. The circles correspond to experimental measurements of the velocity of one grain on a bumpy plane.

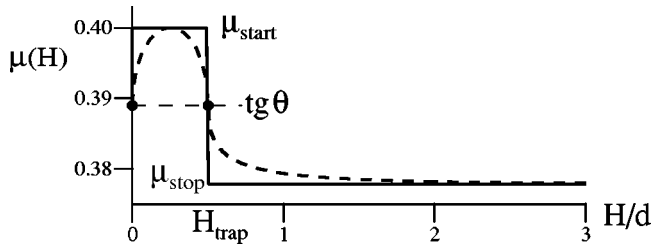


FIG. 4. The flowing layer is globally submitted to an effective friction  $\mu(H)$  which characterizes the force needed to mobilize particles from the static layer of grains. The solid line corresponds to a first order approximation; the dashed one to a regularized version.

as it is equal to the friction coefficient on the rough plane  $\mu_{\text{stop}}(Z=0)$  (Fig. 5). This is clearly a different physical origin.

After the front shape, we can look at the front velocity  $u$ . For a fixed angle, the control parameter is the flux imposed at the top of the plane,  $q_\infty$ . The conservation of matter then fully determines the front velocity  $u = q_\infty / \zeta_\infty$ . Following Pouliquen's results,  $u$  can be rescaled by the gravity  $g$  and the avalanche height  $\zeta_\infty$  to form a Froude number,  $u / \sqrt{g \zeta_\infty}$ , which is plotted for different angles  $\varphi$  as a function of  $\zeta_\infty / Z_{\text{stop}}$  in Fig. 7. The data points obtained for different angles nearly collapse on a single curve, as obtained from the experiments. This rescaling is rather robust toward the details of  $\Gamma(\varphi)$  (Fig. 3) and  $\mu$  (Fig. 4). The rescaled curves exhibit a small curvature as the velocity vanishes when the height  $\zeta_\infty$  tends toward the stopping height  $Z_{\text{stop}}$ . Although reasonable, this last feature was not observed in the experiment. In Pouliquen's scaling law,  $u$  depends on the plane angle  $\varphi$  only through the variation of  $1/Z_{\text{stop}}$  with  $\varphi$ . In our model, the dependence of  $u$  with  $\varphi$  is mostly that of  $\Gamma(\varphi)$ :

$$\frac{u}{\sqrt{g \zeta_\infty}} = \frac{\Gamma(\zeta_\infty - Z_\infty)^2}{2 \cos^2 \varphi \sqrt{g \zeta_\infty}^{3/2}}, \quad (4)$$

where the position  $Z_\infty$  of the static/flowing interface far from

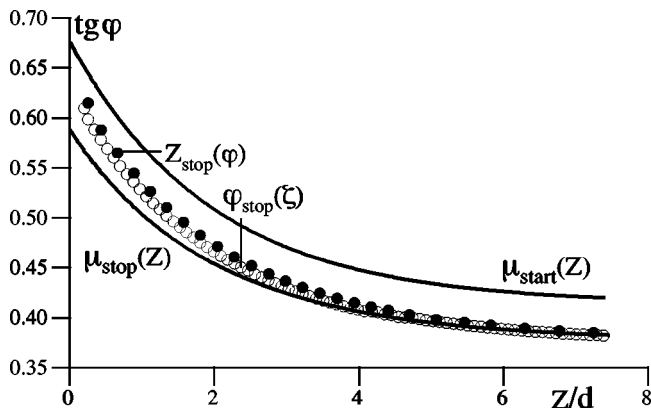


FIG. 5. After an avalanche, a static layer of height  $Z_{\text{stop}}(\varphi)$  remains on the plane (black dots). It is nearly equal, but slightly above the minimum angle  $\varphi_{\text{stop}}$  below which any flow stops (white circles). The friction coefficients  $\mu_{\text{start}}(Z)$  and  $\mu_{\text{stop}}(Z)$  were adjusted to recover the measurement of Pouliquen (system 1).

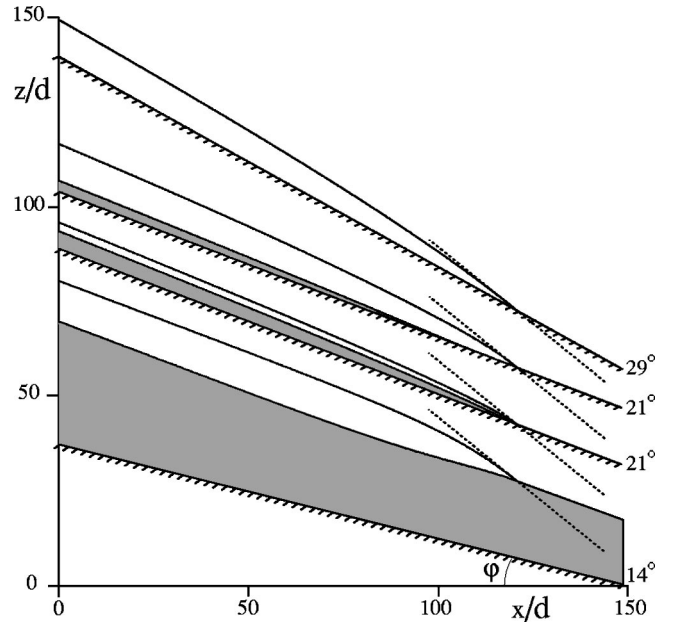


FIG. 6. Front profiles  $\zeta(x)$  for  $\varphi = 14^\circ$ ,  $21^\circ$  (and two flow rates,  $\zeta_\infty = 10d$  and  $\zeta_\infty = 20d$ ) and  $29^\circ$  ( $\zeta_\infty = 15d$ ). The front slope turns out to be constant even for  $\varphi = 14^\circ$  which is equivalent to a free pile, being below  $\varphi_{\text{stop}}^0$ .

the front is determined by the equilibrium between gravity and friction. Now the expression of  $1/Z_{\text{stop}}(\varphi)$  is exactly the one [Eq. (1)] first proposed here for  $\Gamma(\varphi)$ :

$$Z_{\text{stop}} = \sigma d \ln \left( \frac{\tan \varphi_{\text{stop}}^0 - \tan \varphi_{\text{stop}}^\infty}{\tan \varphi - \tan \varphi_{\text{stop}}^\infty} \right). \quad (5)$$

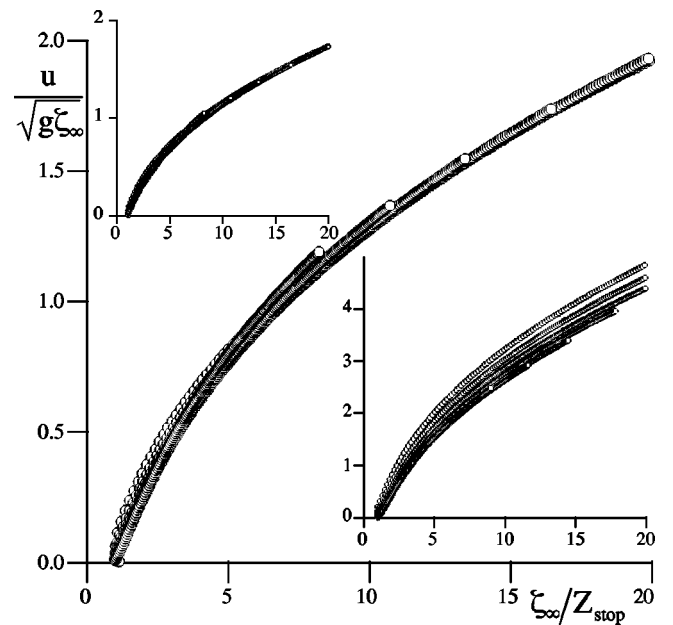


FIG. 7. Froude number  $u / \sqrt{g \zeta_\infty}$  as a function of  $\zeta_\infty / Z_{\text{stop}}$  for different inclination angles (every  $1^\circ$  between  $22^\circ$  and  $28^\circ$ ). Lower right inset: using crude models for  $\Gamma$  and  $\mu$ , with  $\beta = 1.0$ ,  $\theta_0 = 17^\circ$ , and  $\theta_\infty = 35^\circ$ . Upper left inset: same but with adjusted parameters ( $\beta = 0.8$ ,  $\theta_0 = 17^\circ$ , and  $\theta_\infty = 49^\circ$ ). Central figure: using the upper unstable branch for  $\Gamma$  and a regularized friction  $\mu$ , with adjusted parameters ( $\theta_0 = 17^\circ$  and  $\theta_\infty = 32^\circ$ ).

Provided that the two curves  $1/Z_{\text{stop}}(\varphi)$  and  $\Gamma(\varphi)$  are close in the working range of angles ( $22^\circ - 30^\circ$  in Fig. 3), it is natural that the same rescaling occurs.

If they have approximately the same shape,  $1/Z_{\text{stop}}(\varphi)$  and  $\Gamma(\varphi)$  have different meanings:  $Z_{\text{stop}}$  characterizes the bottom effect while  $\Gamma$  relates to the internal equilibrium of the flowing layer, undisturbed by the boundary. They have however one parameter ( $\varphi_{\text{stop}}^\infty$  vs  $\theta_0$ ) of same physical origin which is related to the angle for which a moving grain is eventually trapped by the underneath static ones and which does not depend on the boundary effect. The second parameter ( $\varphi_{\text{stop}}^0$  vs  $\theta_\infty$ ) is that defining the front slope. It has a clear different meaning in the two expressions:  $\theta_\infty$  is the takeoff angle while  $\varphi_{\text{stop}}^0$  is the angle for which no grain can remain on the rough plane. With glued beads as rough plane, these two values are close<sup>7</sup> but they would be very different on a rougher plane: for velvet  $\varphi_{\text{stop}}^0$  increase up to  $50^\circ$  while  $\theta_\infty$  is unchanged. Third, the dependence of  $1/Z_{\text{stop}}(\varphi)$  and  $\Gamma(\varphi)$  with  $d$  insures a perfect rescaling for different bead sizes. The last parameter is the prefactor ( $1/\sigma$  vs  $\beta$ ) which naturally determines the mean slope of the rescaled curves. Now  $\beta$  should vary with the nature of the grains as trapping and collisions are changed. This means that the mean slope of the rescaled curves should be different between for instance glass beads and rough sand.

We have presented an alternative description of avalanches down a rough plane, in which the grains flow only on part of the total height, the rest being static. The rough bottom only makes the grains more difficult to erode near the plane but does not influence the flowing layer, whose rheology, derived from microscopic modeling, is the same than that on a pile. Within this model, we recover the scaling law of the avalanche velocity, which is mainly determined by the variations of the velocity gradient  $\Gamma$ , and the rescaling of the front shape, with a unique front slope with respect to gravity.

Within the same model, we can thus describe continuously the transition from a thick pile to a rough bottom. The interest is then to describe more accurately the way avalanches nucleate, grow from small flowing height, and stop. The model also offers a new interpretation of the rheology of granular flows on a rough plane and suggests several tests to discriminate the possibilities: to compare the fronts slopes on a pile and on a plane; to change radically the roughness of the plane (glass beads over beads and over velvet) and of the grains (sand). If our interpretation was confirmed, it would both give a microscopic understanding of the rheology and extend the use of Pouliquen's type of measurements to any granular surface flow in particular at the surface of sand piles.

<sup>1</sup>O. Pouliquen, "Scaling laws in granular flows down rough inclined planes," *Phys. Fluids* **11**, 542 (1999).

<sup>2</sup>O. Pouliquen, "On the shape of granular fronts down rough inclined planes," *Phys. Fluids* **11**, 1956 (1999).

<sup>3</sup>O. Pouliquen and N. Renaut, "Onset of granular flows on an inclined rough surface: dilatancy effects," *J. Phys. II* **6**, 923 (1996).

<sup>4</sup>A. Daerr and S. Douady, "Two types of avalanche behaviour in granular media," *Nature (London)* **399**, 6733 (1999).

<sup>5</sup>S. Douady, B. Andreotti, and A. Daerr, "On granular surface flow equations," *Eur. Phys. J. B* **11**, 131 (1999).

<sup>6</sup>B. Andreotti and S. Douady, "Selection of velocity profile and flowing depth in granular flows," *Phys. Rev. E* **63**, 031305 (2001).

<sup>7</sup>L. Quartier, B. Andreotti, A. Daerr, and S. Douady, "On the dynamics of a grain on a model sandpile," *Phys. Rev. E* **62**, 8299 (2000).

<sup>8</sup>G. H. Ristow, F. X. Riguidel, and D. Bideau, "Different characteristics of the motion of a single particle on a bumpy inclined line," *J. Phys. I* **4**, 1161 (1994).

<sup>9</sup>D. E. Wolf, "Friction in granular media," in *Physics of Dry Granular Media*, edited by H. J. Hermann *et al.* (Kluwer Academic, Dordrecht, 1998), p. 441.

<sup>10</sup>A. Daerr, "Dynamical equilibrium of avalanches on a rough plane," *Phys. Fluids* **13**, 2115 (2001).

<sup>11</sup>S. Douady, B. Andreotti, A. Daerr, and P. Clade, "The four fronts of the two avalanches," in *Powders and Grains 2001*, edited by Y. Kishino (Balkema, The Netherlands, 2001), p. 443.